Multipoint observations of the open-closed field line boundary as observed by the Van Allen Probes and geostationary satellites during the 14 November 2012 geomagnetic storm

Dixon, Patrick Joseph; MacDonald, E. A.; Funsten, H. O.; Glocer, A.; Grande, Manuel; Kletzing, C.; Larson, B. A.; Reeves, G.; Skoug, R. M.; Spence, H.; Thomsen, M. F.

Published in:
Journal of Geophysical Research: Space Physics

DOI:
10.1002/2014JA020883

Publication date:
2015

Citation for published version (APA):
Dixon, P. J., MacDonald, E. A., Funsten, H. O., Glocer, A., Grande, M., Kletzing, C., Larson, B. A., Reeves, G., Skoug, R. M., Spence, H., & Thomsen, M. F. (2015). Multipoint observations of the open-closed field line boundary as observed by the Van Allen Probes and geostationary satellites during the 14 November 2012 geomagnetic storm. *Journal of Geophysical Research: Space Physics*, *120*(8), 6596-6613. https://doi.org/10.1002/2014JA020883

AGU PUBLICATIONS

JGR

Journal of Geophysical Research: Space Physics

RESEARCH ARTICLE
10.1002/2014JA020883

Special Section:
New perspectives on Earth's radiation belt regions from the prime mission of the Van Allen Probes

Multipoint observations of the open-closed field line boundary as observed by the Van Allen Probes and geostationary satellites during the 14 November 2012 geomagnetic storm

P. Dixon[1], E. A. MacDonald[2], H. O. Funsten[3], A. Glocer[2], M. Grande[1], C. Kletzing[4], B. A. Larsen[3], G. Reeves[3], R. M. Skoug[3], H. Spence[5], and M. F. Thomsen[3]

[1]Department of Physics, Aberystwyth University, Wales, UK, [2]NASA Goddard Space Flight Center, Greenbelt, Maryland, USA, [3]Los Alamos National Laboratory, Los Alamos, New Mexico, USA, [4]Department of Physics and Astronomy, University of Iowa, Iowa City, Iowa, USA, [5]Department of Physics, University of New Hampshire, Durham, New Hampshire, USA

P. Dixon and E. A. MacDonald contributed equally to this work.

Key Points:
- Observations consistent with lobe encounters by multiple spacecraft
- Disturbances on the open-closed field line boundary propagating from the tail
- Novel data-model comparison method shows some agreement on boundary dynamics

Correspondence to:
P. Dixon,
pjd9@aber.ac.uk

Citation:
Dixon, P., et al. (2015), Multipoint observations of the open-closed field line boundary as observed by the Van Allen Probes and geostationary satellites during the 14 November 2012 geomagnetic storm, *J. Geophys. Res. Space Physics*, *120*, 6596–6613, doi:10.1002/2014JA020883.

Received 28 NOV 2014
Accepted 19 MAY 2015
Accepted article online 25 MAY 2015
Published online 31 AUG 2015

Abstract The twin Van Allen Probes spacecraft witnessed a series of lobe encounters between 0200 and 0515 UT on 14 November 2012. Although lobe entry had been observed previously by other spacecraft, the two Van Allen Probe spacecraft allow us to observe the motion of the boundary for the first time. Moreover, this event is unique in that it consists of a series of six quasi-periodic lobe entries. The events occurred on the dawn flank between 4 and 6.6 local time and at altitudes between 5.6 and 6.2 RE. During the events *Dst* dropped to less than −100nT with the IMF being strongly southward ($B_z = -15$nT) and eastward ($B_y = 20$ nT). Observations by LANL-GEO spacecraft at geosynchronous orbit also show lobe encounters on the dawn and dusk flanks. The two spacecraft configuration provides strong evidence that these periodic entries into the lobe are the result of local expansions of the OCB propagating from the tail and passing over the Van Allen Probes. Examination of pitch angle binned data from the HOPE instrument shows spatially large, accelerated ion structures occurring near simultaneously at both spacecraft, with the presence of oxygen indicating that they have an ionospheric source. The outflows are dispersed in energy and are detected when the spacecraft are on both open and closed field lines. These events provide a chance to examine the global magnetic field topology in detail, as well as smaller-scale spatial and temporal characteristics of the OCB, allowing us to constrain the position of the open/closed field line boundary and compare it to a global MHD model using a novel method. This technique shows that the model can reproduce a periodic approach and retreat of the OCB from the spacecraft but can overestimate its distance by as much as 3 R_E. The model appears to simulate the dynamic processes that cause the spacecraft to encounter the lobe but incorrectly maps the overall topology of the magnetosphere during these extreme conditions.

1. Introduction

Previous observations of spacecraft near geosynchronous altitudes moving between regions of open and closed field lines have been shown to be either magnetopause crossings [*Wrenn et al*., 1981; *McComas et al*., 1994] or tail-lobe entries [e.g., *Sauvaud and Winckler*, 1980; *Thomsen et al*., 1994]. Magnetopause crossings are only observed at geosynchronous orbit on the dayside of the magnetosphere, whereas lobe encounters have been observed at most local times [*Moldwin et al*., 1995]. Lobe encounters are characterized by a rapid decrease of particle fluxes to background levels at energies from 1 eV to 40 keV [*McComas et al*., 1993], followed by a rapid recovery to previous levels. A strong, stretched and taillike field is also seen when crossing into the lobes [*Fennell et al*., 1997], especially during times of increased geomagnetic activity and southward IMF [*Kopányi and Korth*, 1995].

Moldwin et al. [1995] defined tail-lobe entry events as fitting into two distinct classes, those that occurred around local midnight and those that occur on the flanks of the magnetosphere. The former are associated with stretching of the near-Earth field, leading to thinning of the plasma sheet, during a substorm growth phase, and the latter with large-scale reconfigurations caused by unusual IMF strength and orientation, i.e., very strong B_z or B_y. Flank lobe encounters have been observed by spacecraft as low as ~3° south in magnetic latitude at 6.6 R_E [*Kopányi and Korth*, 1995] and above 10° both north and south of the magnetic equator [*Fennell et al*., 1997]. Lobe encounters have a tendency to occur in groups, with

one statistical survey finding two thirds of lobe entry events occurring within 24 h of another over a period of 4 years [*Moldwin et al*., 1995]. Multiple studies [e.g., *Thomsen et al*., 1994; *Moldwin et al*., 1995; *McComas et al*., 1994] have shown a preference for lobe encounters to occur in the morning sector of the magnetosphere, with suggested causes being an asymmetry in the rate of reconnection [*Thomsen et al*., 1994] or an unbalanced inflation of the magnetosphere on the dusk side, caused by an asymmetry in the storm-time ring current [*McComas et al*., 1994].

Encounters with the lobe at or near geosynchronous orbit have been found to coincide with periods of strong disturbance caused by extreme IMF conditions, which lead to large-scale reconfigurations of magnetosphere geometries [*Thomsen et al*., 1994]. The occurrence of these events during very strong IMF B_y has been previously simulated [*Moldwin et al*., 1995] by modifying the Tsyganenko T87 model to show what the expected magnetic field topology should be during these conditions. An asymmetry was found in the magnetic field configuration which predicts that regions of open field lines should be brought closer to geosynchronous orbit for southern dawn and northern dusk sectors for negative B_y and the reverse for positive B_y. These magnetospheric reconfigurations combined with a large geomagnetic storm are proposed as the cause of the majority of flank lobe encounters. However, a subsequent statistical study of numerous events did not show this B_y pattern unequivocally (M. Thomsen, personal communication, 2013).

Spacecraft encountering the magnetospheric lobe must cross the open-closed field line boundary (OCB), which is the separation between closed field lines having both footpoints in the Earth's ionosphere and open field lines which have one footpoint in the solar wind. The OCB is readily determined in physics-based magnetohydrodynamic models and can be compared to in situ observations [e.g., *Kabin et al*., 2004; *Aikio et al*., 2008; *Rae et al*., 2004]. A variety of techniques exist to probe the open-closed boundary remotely using radars, magnetometers, and optical instrumentation [e.g., *Aikio et al*., 2006; *Amm*, 1997, 1998; *Chisham et al*., 2005; *Clausen et al*., 2013; *Urban et al*., 2011]. The OCB is critical to numerous topics in space physics, including the mechanisms and mapping of MHD models, planetary magnetospheres, and magnetosphere-ionosphere coupling. Magnetic mapping problems are of critical importance to magnetosphere-ionosphere coupling and geospace systems science. Global MHD models may represent the most self-consistent method of mapping [*Paschmann et al*., 2003]; however, mapping remains extremely challenging during storms and over long distances.

In this paper observations of multiple lobe encounters by the two Van Allen Probe satellites and several geosynchronous satellites during an interval of high geomagnetic activity are used to examine OCB mapping at the flanks of the magnetosphere. Multipoint in situ observations and global MHD models are compared. In addition, the Van Allen Probe observations enable two additional important findings: First, the co-orbiting dual spacecraft allow us to examine the evolution of the OCB, and second, the ion composition capability allows us to explore the nature and source of a low-energy, field-aligned ion flow that has been previously noted in such events, but not examined [*Moldwin et al*., 1998].

1.1. Instrumentation and Models Used

The Van Allen Probes mission, formerly known as the Radiation Belt Storm Probes (RBSP) mission [*Kessel et al*., 2013; *Mauk et al*., 2013], is designed and exquisitely instrumented to probe the mysteries of the magnetosphere. Two spacecraft, launched together in 2012, have similar 9 h low inclination (10°) orbits and lap each other every 75 days. Their apogee is 5.8 R_E and their perigee is 1.1 R_E. At the time of this paper's interest, the spacecraft had their apogee in the dawn sector and were relatively close together. They were ideally located to observe extreme stretching during the 14 November 2012 geomagnetic storm. The Van Allen Probes carry an identical and comprehensive suite of instruments designed to measure all waves and particles of interest in the harsh background of the radiation belt environment with higher sensitivity than any previous mission. Instruments utilized in this paper include the Helium Oxygen Proton Electron (HOPE) spectrometer, part of the Energetic Composition and Thermal (ECT) particle suite, and the Electric and Magnetic Fields Instrument Suite and Integrated Science (EMFISIS) [*Spence et al*., 2013; *Kletzing et al*., 2013].

The HOPE spectrometer was designed and built at Los Alamos National Laboratory and uses a top-hat electrostatic analyzer to measure both positive and negative species from 1 eV to 50 keV [*Funsten et al*., 2013]. During the event studied here the minimum energy was 25 eV. Ten channel electron multipliers

(CEMs) are used as start and stop detectors, and the coincidence and time-of-flight is recorded to reduce the background rate from penetrating radiation and to provide species identification.

Data are also utilized from the Los Alamos National Laboratory geosynchronous spacecraft energetic particle instrument Synchronous Orbit Particle Analyzer (SOPA) on board the spacecraft in operation at the time of the event: LANL-080, LANL-084, LANL-97A, LANL-01A, LANL-02A, and LANL-04A. The satellites operate at geosynchronous orbit (6.6 R_E) at the geographic equator with a 24 h orbital period, giving a fixed longitude and a nominal magnetic latitude of up to 11°. The spacecraft have a spin period of 10.24 s with the spin axis actively controlled to point toward the center of the Earth. The SOPA instrument measures electrons from 50 keV to 26 MeV over 16 energy channels and protons from 50 keV to >50 MeV over 15 energy channels [*Belian et al*., 1992]. Though the Magnetospheric Plasma Analyzer (MPA) instrument has similar energies to the HOPE instrument, MPA flux data were not publicly available at the time of this writing; however, the dropouts occur over a wide range of energies so this is not expected to impact the subsequent analysis.

Simulated magnetospheric data were obtained using the CRCM + BATS-R-US coupled global MHD and ring current model implemented in *Glocer et al*. [2013]. In this study the Block-Adaptive-Tree Solar-Wind Roe-Type Upwind Scheme (BATS-R-US) model is configured to solve ideal MHD equations, using a Cartesian grid. The domain of the modeled magnetosphere ranges from 32 R_E sunward to 224 R_E tailward and 64 R_E to the sides of the Earth, with an inner boundary 2.5 R_E from the planet. The resolution of the simulation varies from 1/8 R_E in the inner magnetosphere to 4 R_E at the edges of its domain. The Comprehensive Ring Current Model (CRCM) simulates the ring current electrons and ions by solving the bounce averaged Boltzmann transport equation described in *Fok et al*. [1995]. The domain of the model is defined by the ionospheric foot point of its field lines and the distance of the last closed field line, extending no further than 15 R_E from the Earth. It is important to note that the ionospheric outflow model, such as PWOM [*Glocer et al*., 2009], was not used in this simulation.

The two models are coupled together using the Space Weather Modeling Framework described by *De Zeeuw et al*. [2004]. Information from field lines whose footpoints are within the CRCM grid are extracted from BATS-R-US and passed to CRCM along with equatorial mass density and thermal pressure at the model boundary. CRCM then uses these data along with ionospheric potential obtained from a height-integrated conductance model and potential solver [*Ridley et al*., 2004] to calculate ring current fluxes, density, and parallel and perpendicular pressure. These values are then fed back to BATS-R-US and used to nudge its values in the inner magnetosphere toward those provided by CRCM over a short period of time (typically 20 s). The present runs use a version of BATS-R-US that solves the anisotropic MHD equations. As such the coupling is able to account for pitch angle anisotropy in the coupling as described by *Meng et al*. [2013].

2. Event Conditions

The period of interest (0100–0600 UT on 14 November 2012) occurs during the main phase of a moderate geomagnetic storm (minimum $Dst = -108$ nT) and during a period of highly disturbed interplanetary magnetic field (IMF) conditions observed by the ACE spacecraft at L1 (Figure 1). Prior to the commencement of the storm, at 2230 UT 12 November 2012 ACE detected a C-type CME followed by rapidly fluctuating IMF conditions before a period of very strong, persistent IMF B_y (+20 nT) and a rotation of IMF B_z from northward to southward beginning at approximately 0900 UT 13 November 2012. IMF B_z becomes southward at 1700 UT and stays southward until 0900 UT the next day, after the period examined is over. Solar wind speed was nearly constant at ~380 km/s for 12 h prior to the events. There was a large increase in proton density starting at 0212 UT on 14 November and peaking at 21 particles/cm^3 at 0357 UT.

Both the IMF B_y and B_z are unusually large, taking on their highest values in several months. These conditions, consistent with those seen in *Moldwin et al*. [1995] and *Thomsen et al*. [1994], would cause a build-up of flux in the lobes via reconnection and would cause the lobes to be highly skewed in the y direction. There are no clear IMF signatures relating to the individual events for any of the solar wind parameters, though shortly after the onset of the events the IMF conditions change dramatically with B_x and B_y beginning to fluctuate.

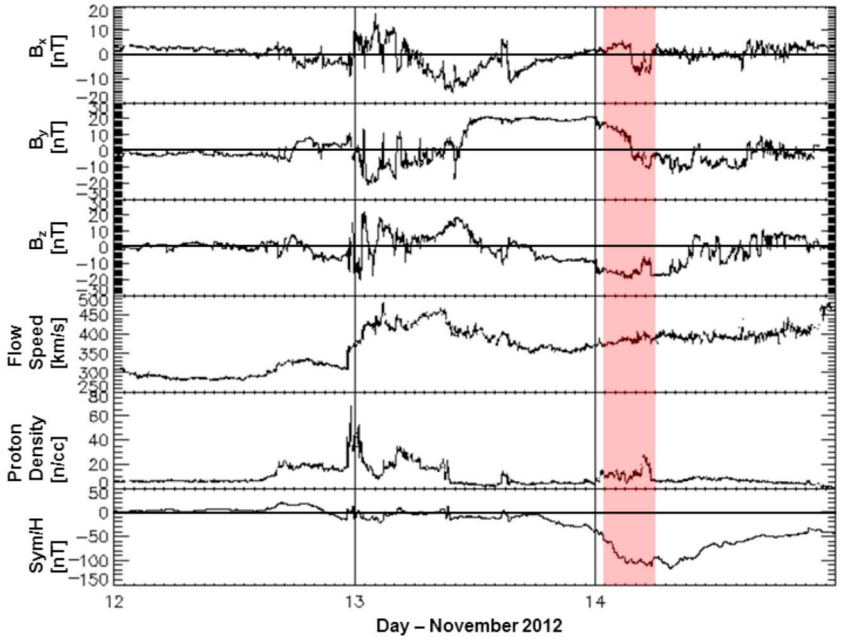

Figure 1. Solar wind data from the ACE spacecraft with times shifted to account for distance for L1 to the magnetosphere for the 12–14 of November 2012. The period examined in this work, 0100–0600 14 November 2012, is highlighted in red. At approximately 2300 12 November 2012, a CME can be seen reaching the magnetosphere. Data were obtained and plotted from the NASA OMNIWEB service.

Over a 5 h period on 14 November 2012 the twin Van Allen Probes observed multiple rapid decreases and then recoveries of particle fluxes over almost the whole energy range of the HOPE instrument, from tens of eV to 50 keV. Figure 2 shows differential ion and electron fluxes from the HOPE instruments aboard RBSP-A and RBSP-B for the period of 0100–0600 UT on 14 November 2012. Events 1–5 are seen by RBSP-A shown in Figures 2a, 2c, 2e, and 2g and events 2–6, seen by RBSP-B, are shown in Figures 2b, 2d, 2f, and 2h. For each event the plasma fluxes for both positive and negative species sharply drop several orders of magnitude to background levels, before rapidly recovering to their previous state minutes later. There is some structure within each dropout, particularly for events 4 and 5, where the particle fluxes very briefly recover to levels seen outside the events. There is no overall change in particle fluxes after each event as compared to before, which is consistent with the spacecraft having moved between two different plasma populations. Figure 2 also shows large (50 nT) increases and then decreases in magnetic field strength, observed by the magnetometer in the EMFISIS instrument suite between 0100 and 0600. Figure 2i shows EMFISIS data from RBSP-A, and Figure 2j shows EMFISIS data from RBSP-B. These observations coincide with the flux dropouts seen by the HOPE instrument, both for the start and end times of each event and also some of the finer structure within them. The magnetic field for this entire orbit is abnormally strong, highly stretched and not very dipolar. These particle and magnetic field signatures appear wholly consistent with those seen in previous investigations during the CRRES era of spacecraft near geosynchronous orbit crossing the open-closed field line boundary (OCB), entering the lobe and crossing back to the closed field region a short time later [e.g., *Moldwin et al.*, 1995; *Thomsen et al.*, 1994; *Fennell et al.*, 1996].

During this time period four of the six LANL-GEO geosynchronous satellites also observed dropouts of electron and proton fluxes consistent with lobe entries. Figure 3 shows proton flux data from the SOPA instrument aboard the four LANL-GEO spacecraft that saw flux dropouts between 0100 and 0600 UT. Fluxes from the six lowest energy channels with an overall range of 50–670 keV are used. This does not overlap with the energy range of HOPE (25 eV–50 keV) but examination of higher energy ion and electron data from the RBSPICE [*Mitchell et al.*, 2013] and MagEIS [*Blake et al.*, 2013] instruments aboard the Van Allen Probes shows that the flux dropouts they observe extend up to energies similar to those seen by SOPA. Three lobe encounters seen by LANL-97A occurred at very similar times and magnetic local times to

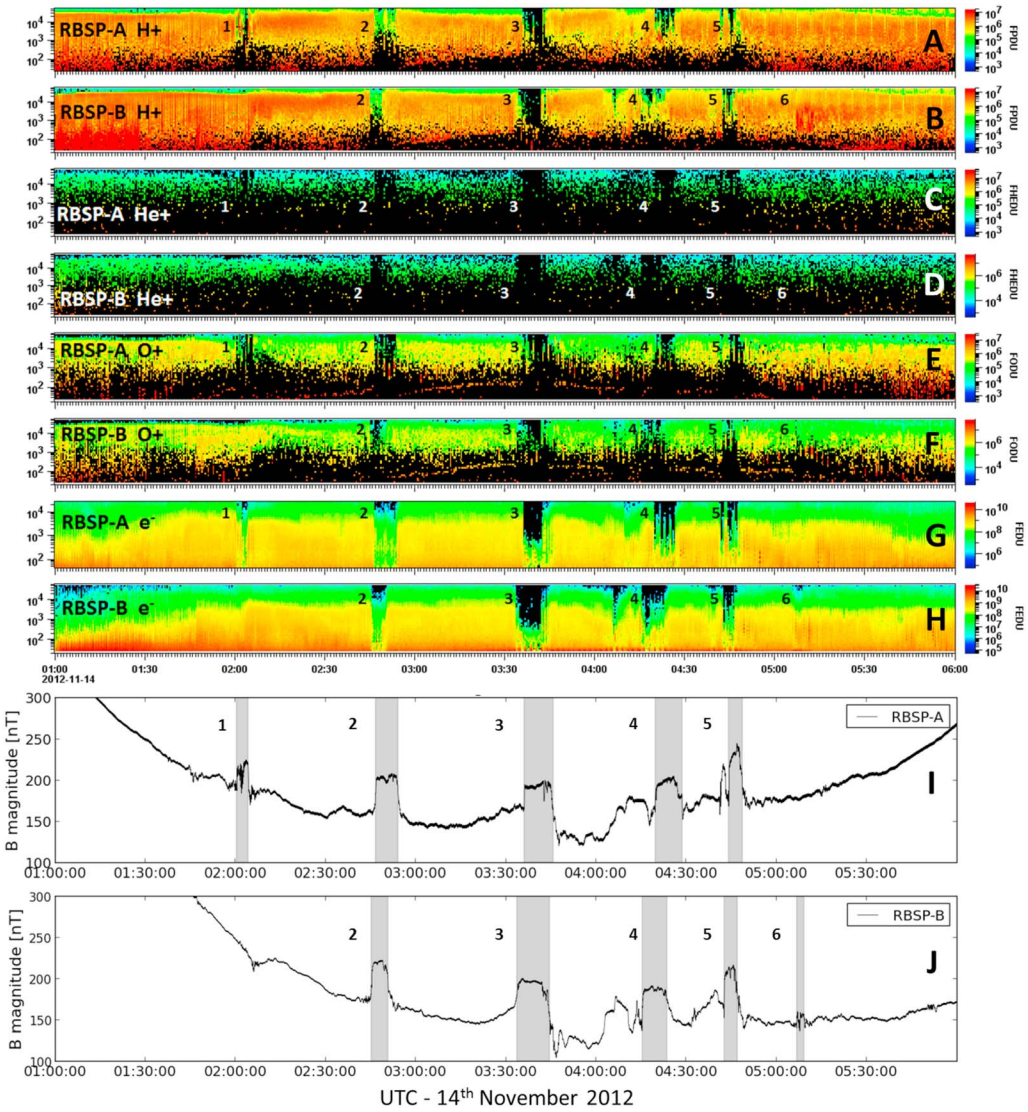

Figure 2. Van Allen Probes particle flux and magnetic field data showing multiple flux dropouts and magnetic field strength increases between 0100 and 0600 on 14 November 2012. (a–h) HOPE differential particle fluxes for RBSP-A and RBSP-B over an energy range of eV to 50 keV, with the events seen by each spacecraft numbered 1–6. (i and j) Magnetic field strength detected by the EMFISIS magnetometer over the same period. Each event is highlighted in grey and numbered similarly to the particle fluxes.

encounters 1, 3, and 5 seen by the Van Allen Probes; they have been given the same label. The rest of the LANL-GEO spacecraft lobe entries have been labeled in order of increasing magnetic local time (MLT).

In total there are 20 entries into the lobe seen over five spacecraft in the southern dawn (RBSP-A, RBSP-B), northern dawn (LANL-97A), and southern dusk (1991–080 and LANL-01A) sectors of the magnetosphere. These entries vary in duration from a few minutes to almost an hour, with the two spacecraft in the southern dusk sector seeing significantly longer entries than the others. The lobe entry times and durations are summarized in Table 1 and derived by the following method.

Each Van Allen Probes boundary crossing is identified by a sharp drop in particle flux (seen in all ions and the electrons) accompanied by a sharp increase in the magnetic field strength. As the magnetic field strength measurements consist of a sharper boundary, they are chosen to identify the start and end points of each event. For consistency the onset and recovery time of each event is defined as the time at which the magnetic field magnitude is halfway through its increase or decrease, e.g., if the magnetic field strength rose from 150 nT to 210 nT, then the onset would be defined as the time at which it reached 180 nT.

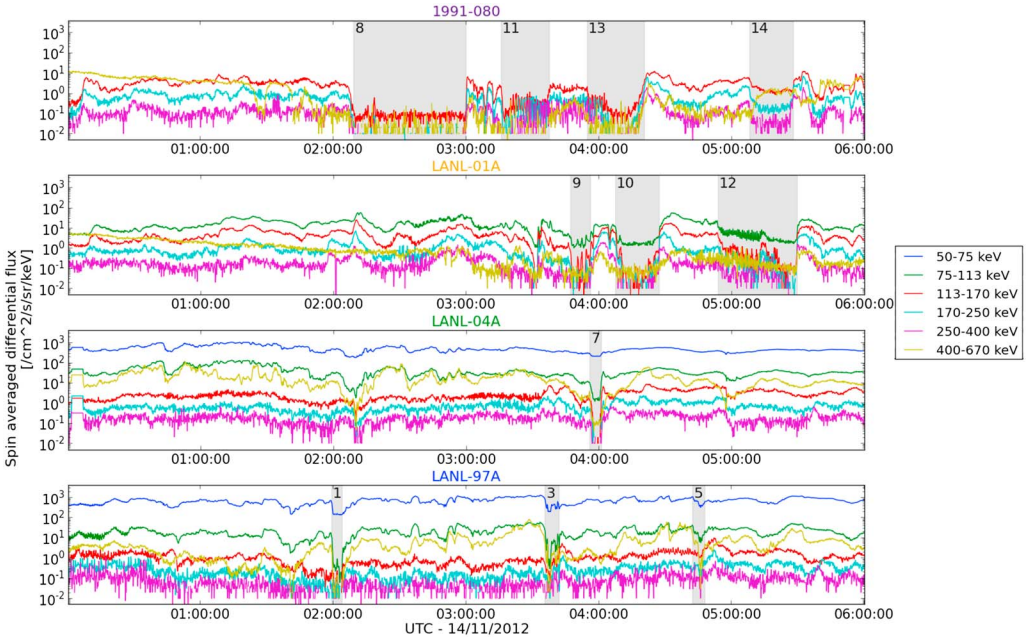

Figure 3. LANL-GEO spin averaged differential proton fluxes from the SOPA instrument. Six energy bands are shown from 50 to 670 keV. Grey-shaded areas highlight lobe entries. Spacecraft 1991–080 and LANL-01A, situated in the dusk region of the magnetosphere, are shown in the top two panels. LANL-04A and LANL-97A situated in the dawn region are shown in the bottom two panels. Spacecraft 1994–084 and LANL-02A did not encounter the lobe and are not shown.

Event 6, seen only by RBSP-B, has a significantly smaller increase in magnetic field strength compared to the other events, with the drop in particle fluxes also being particularly small. The magnetic field observations for this event still show the sharp increase and then rapid decline seen for the other events and so it is included as a valid event, despite its relative weakness.

For the LANL-GEO spacecraft a slightly different approach was taken as they are not equipped with onboard magnetometers and the event times cannot be ascertained from changes in magnetic field strength. Instead

Table 1. Lobe Crossing Times Between 0100 and 0600 UT on 14 November 2012[a]

	Start/End Times (UT)	Δt	Label
RBSP-A	02:00:27–02:04:17	3 m 50 s	1
	02:46:40–02:54:09	7 m 29 s	2
	03:36:07–03:45:45	9 m 38 s	3
	04:19:42–04:28:42	9 m	4
	04:44:14–04:48:43	4 m 29 s	5
RBSP-B	02:45:19–02:50:45	5 m 26 s	2
	03:33:37–03:44:39	11 m 2 s	3
	04:15:19–04:23:33	8 m 14 s	4
	04:42:37–04:47:01	4 m 24 s	5
	05:06:45–05:09:19	2 m 34 s	6
LANL-97A	01:59:29–02:04:11	4 m 42 s	1
	03:35:53–03:42:11	6 m 18 s	3
	04:42:35–04:47:51	5 m 16 s	5
1991-080	02:09:15–02:59:59	50 m 44 s	8
	03:15:57–03:37:47	20 m 50s	11
	03:54:52–04:20:43	25 m 51 s	13
	05:08:18–05:27:56	19 m 38 s	14
LANL-01A	03:47:04–03:56:07	9 m 3 s	9
	04:07:34–04:27:12	19 m 38 s	10
	04:53:46–05:29:27	35 m 41 s	12
LANL-04A	03:55:54–04:00:58	5 m 4 s	7

[a]Events that overlap in time are given the same number.

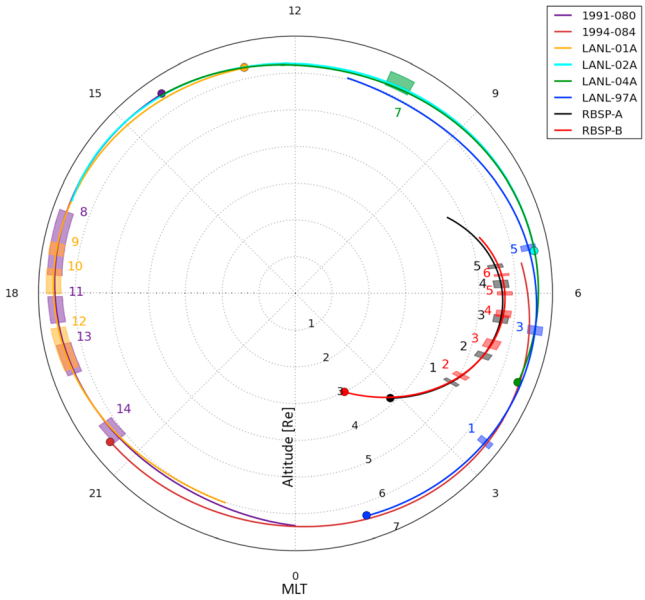

Figure 4. Polar plot of magnetic local time (MLT) and altitude for the orbits of the Van Allen Probes and six LANL-GEO spacecraft. Spacecraft orbits shown for the period 0100–0600 with the times at which they entered the lobe marked by shaded boxes on their orbit line. All orbits are forward in MLT, and the start of each is marked by a circle. Lobe encounter events are numbered in ascending MLT with full details in Table 1. Note that 1994–084, situated near midnight, and LANL-02A, situated near noon, did not encounter the lobe.

the changes in proton flux in the 75–113, 113–170, and 170–250 keV channels of the SOPA instrument were examined. A similar procedure to that used above for the Van Allen Probes magnetometer data was implemented to identify the start and the end of each flux dropout. The midpoints of each sharp decrease and increase in flux are calculated, and the mean times for the three energy channels found. This accounts for the small differences seen in start and end times of the dropouts for the different energy levels.

3. In Situ Lobe Location Analysis

Figure 4 shows a polar plot of magnetic local time (MLT) against altitude for all six of the LANL-GEO geosynchronous spacecraft and the twin Van Allen Probes. The colored lines show the orbit of each spacecraft over a 5 h period from 0100 to 0600 UT, and the shaded boxes show the periods at which each spacecraft entered the lobe. The colored circles mark the start time at each spacecraft's orbit. For lobe encounters 1, 3, and 5, it can be seen that LANL-97A is at a similar MLT to the Van Allen Probes when it encounters the lobe. For the dusk spacecraft, 1991–080 and LANL-04A, the lobe encounters mostly occur between 16.5 and 19.5 MLT. The overlap of the shaded boxes shows that the lobe encounters happened in similar regions of space but at significantly different times, e.g., event 9 happens about 90 min after event 8.

It is also critically important to consider magnetic latitude to understand the global context of this event. Figure 5 shows the magnetic latitudes of the five spacecraft between 0100 and 0600 UT. These magnetic latitudes are determined from the Van Allen Probes SOC magnetic ephemeris files in the following way. The Tsygenanko 2004 (TS04) magnetic field model is used for the external field, while the IGRF is used for

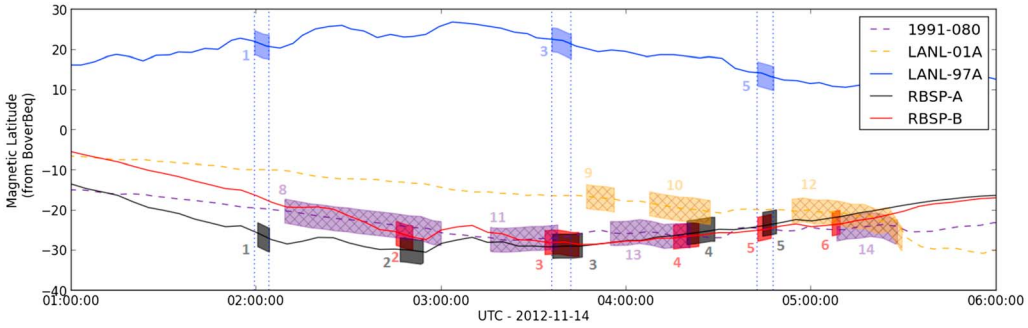

Figure 5. Magnetic latitudes estimated from Tsyganenko TS04 magnetic field calculations. Shaded boxes show durations of lobe entries for each spacecraft. Dashed lines/hatched boxes mark the two spacecraft (1991–080 and LANL-01A) that are on the dusk side of the magnetosphere. The dotted vertical lines are used to highlight the similarity in time between the three events seen by LANL 97-A in the northern hemisphere and lobe encounters 1, 3, and 5 seen by the Van Allen Probes in the southern hemisphere.

the internal [*Tsyganenko and Sitnov*, 2005]. The TS04 model traces the field line connected to the spacecraft trajectory at each time step and determines the minimum magnetic field along that field line. From the ratio of the magnetic field at the spacecraft to the minimum magnetic field, the magnetic latitude at the spacecraft is estimated. The shaded boxes show the times at which the spacecraft are inside the lobe, and it should be noted that the height of each box does not represent an extent in magnetic latitude. The two spacecraft on the dusk side of the magnetosphere are differentiated by dashed lines and hashed boxes. The vertical, dotted, blue lines are used to highlight the strong correlation between the lobe encounters seen by LANL-97A and the first, third, and fifth encounters seen by the Van Allen Probes. There are also small reductions in flux seen by LANL-97A at the same time as the second and fourth events, but these are difficult to discern and cannot reliably be defined as a lobe crossing.

It can be seen that the Van Allen Probes reach greater absolute magnetic latitude (~ −30°) in the southern hemisphere than LANL-97A does in the northern hemisphere (~25°). Before 0400 RBSP-A is at higher absolute magnetic latitude than RBSP-B with the difference largest (~10°) for the first lobe encounter and gradually getting smaller as the spacecraft reach apogee. After apogee, RBSP-B is at slightly more southerly magnetic latitudes than RBSP-A.

The two spacecraft in the southern dusk region (1991–080 and LANL-01A) experienced the most prolonged and complete entries into the lobe, with 1991–080 measuring a drop in flux to background levels for a period of approximately 50 min.

Spacecraft 1991–084 and LANL-02A situated around midnight and late morning, respectively, did not experience any clear entries into the lobes, which is not unusual for spacecraft in those regions. LANL-04A does experience a dropout and recovery of flux at 0355 and ~10 MLT, but its position near to noon means this flux dropout could be an encounter with the magnetopause rather than the lobe. The model of *Shue et al*. [1997] shows the magnetopause being compressed to ~7.5 R_E at this time but only has a resolution of an hour.

Previous work by *Moldwin et al*. [1995] suggested there should be a preference for entries into the lobe at geosynchronous orbit in the southern dusk and northern dawn regions due to the strong positive IMF B_y seen before the events. This is supported partly by the prolonged lobe entries seen in the southern dusk region but not by the events seen in the southern dawn and the relative weakness of those seen at northern dawn. These mixed results suggest that though the strength and orientation of IMF B_y may be a factor in where geosynchronous spacecraft can access the lobes, factors such as seasonal variations, solar wind conditions, and storm-time dynamics also play a role.

These multiple encounters into the southern and northern lobes in both the dawn and dusk regions of the magnetosphere suggest that the movement of the OCB is a global phenomenon. Though there may be small-scale local phenomena occurring near the spacecraft, the expansion of the lobes which makes them more accessible to the spacecraft occurs across most of the magnetosphere at very similar times. These spatial and temporal results can be compared with global boundaries obtained from modeling techniques. Here we will present results obtained using the CRCM + BATS-R-US global MHD model.

Figure 6 shows some example frames of the open-closed field line location data visualization obtained from CRCM + BATS-R-US. The model differentiates between regions of open and closed field lines, with the open field line of the northern and southern lobes colored green and yellow and the closed field lines of the equatorial region colored red. A subset of the global magnetospheric data produced by the model is used here, with each data point situated on the surface of a sphere at 6.6 R_E. This figure shows 1991–080 and LANL-01A (situated at dusk) spacecraft, as well as portions of the orbits of 1994–084 (situated around midnight) and LANL-02A (situated around noon). The first frame, taken at approximately 0140 UT, shows 1991–080 within the southern lobe and LANL-01A situated just outside it in a region of closed field lines. The second frame, taken at 0340 UT, shows LANL-01A inside the lobe and 1991–080 having just crossed the OCB back onto closed field lines. Between the second and third frames there is a large retreat of the lobe to higher negative magnetic latitudes, greatly increasing the distance between the spacecraft and the OCB. These examples qualitatively show that for the dusk spacecraft the model predicts that the spacecraft would have access to the lobe at times during this period. They also highlight both the large-scale motions of the boundary, e.g., the retreat of the southern lobe after 0340 UT, and the smaller-scale topological changes that can be seen along the boundary between each frame.

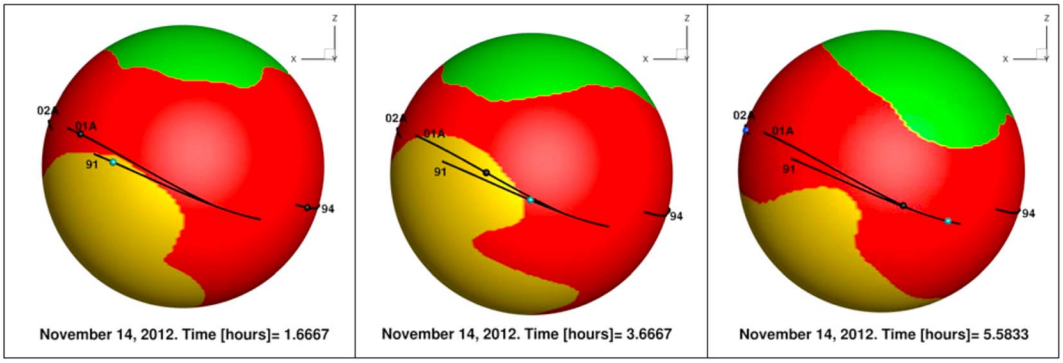

Figure 6. CRCM + BATS-R-US model data showing the locations of regions of open and closed field lines at 6.6 R_E. The red area represents the equatorial region of closed field lines, the green area the open field lines of the northern lobe, and the yellow area the open field lines of the southern lobe. The snapshots are taken from a dusk perspective and show the orbits of the two spacecraft situated in this region, 1991–080 (abbreviated to "91" in the figure) and LANL-01A (abbreviated to "01A"). Partial orbits of LANL-02A ("02A"), situated around noon, and 1994–084 ("94"), situated around midnight, are also shown.

The multiple encounters with the magnetospheric lobe seen by the LANL-GEO geosynchronous spacecraft and the Van Allen Probes allow us to constrain the position of the open-closed field line boundary and compare it to the predicted position obtained through simulation. The model temporal resolution of the output is 5 min, compared to 10.9 s for the HOPE instrument aboard the Van Allen Probes and 10 s for SOPA aboard the LANL-GEO spacecraft. This means the comparison can only be done at 5 min intervals with each time frame in the model being matched to the spacecraft data point which is closest to it in time. Similarly the model only has a spatial resolution of about 0.1–0.2 R_E in this region of the magnetosphere so there may be some error due to interpolation inside the coarse grid. At each time step of the spacecraft trajectory moving through the model, the region of space nearby is searched for the nearest lobe boundary. When the lobe boundary is found the magnitude of the vector between the spacecraft trajectory point and the lobe boundary is reported. For numerical efficiency the exact method to find the lobe boundary expands a series of spheres around each trajectory point. Field lines are traced starting at each point on the surface of a given sphere and the corresponding magnetic topology is determined. When the spacecraft is on a closed (open) field, a very small sphere will only have closed (open) topologies present on the surface. As the sphere gradually increases in size, it will eventually touch the surface defining the open-closed boundary and more than one topology type will be found on the sphere. The radius of the sphere then defines the distance from the spacecraft to the open-closed boundary. To make the calculation of the distance even more efficient, we use a bisection method rather than simply step radially outward with small steps.

Thus, we derive, between 0100 and 0600 UT, how far away the MHD model says the lobe boundary is from the spacecraft. When the model and the in situ data agree about being in the lobes, this is reflected as a (nonphysical) separation of less than 0 R_E and the nominal interpretation is that this good agreement represents accurate mapping of the open-closed boundary in the model. We present these results for each region, starting at dusk. Figure 7 shows the calculated distance to the OCB for the two spacecraft in the southern dusk region, 1991–080 (purple) and LANL-01A (yellow). The thick lines show the times at which the spacecraft data indicated they had passed into the lobe. Events 8 and 11 seen by LANL-080 and 9 seen by LANL-01A occur at times when the model predicts the spacecraft would be either very close to or inside the lobe. This represents the most consistent data-model comparison.

At around 0400 UT the model shows the southern lobe contracting back to higher latitudes, increasing the distance to the OCB to over 3 R_E and 1 R_E for 1991–080 and LANL-01A, respectively. This large change in the topology of the magnetosphere coincides with the change in IMF B_y from positive to negative. Events 10 and 12 seen by LANL-01A also occur after the OCB retreats, but due to LANL-01A being behind 1991–080 by approximately 90 min of MLT and the specific topology of the boundary, LANL-01A stays in closer proximity to the lobe. For both events there seems to be a movement of the boundary toward the spacecraft, with the model showing it being within 0.5 R_E of the spacecraft for event 10. Event 13 occurs as the boundary begins

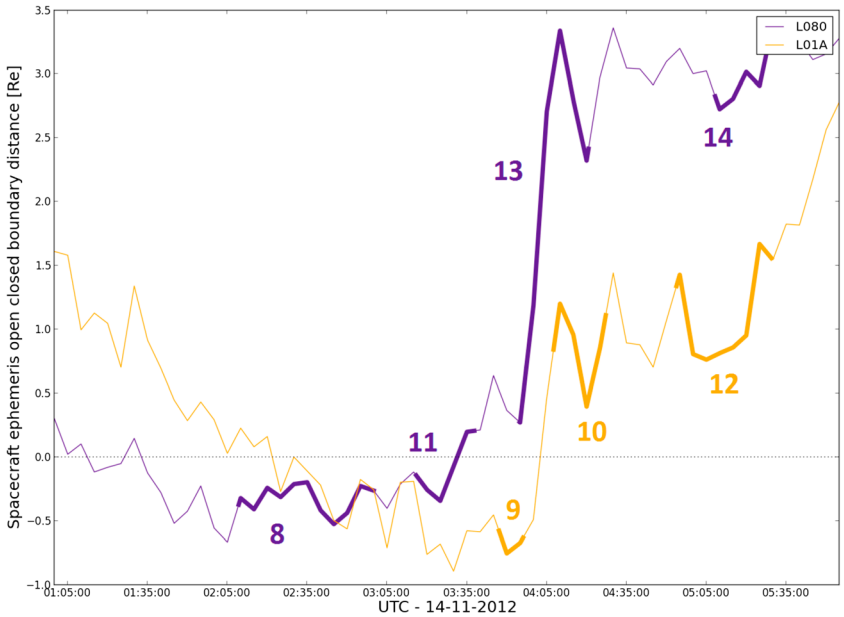

Figure 7. Calculated distances from 1991–080 (purple) and LANL-01A (gold) to the open-closed field line boundary position predicted by CRCM + BATS-R-US. Distances shown are in R_E with negative distance representing when the spacecraft has entered the lobe. Thicker lines show periods where the spacecraft data indicate that it has entered the lobe.

to retreat from the spacecraft, and event 14 once it has retreated to a distance of ~3 R_E. For the seven observed lobe encounters in the dusk sector, six show some agreement with the model prediction to within ±1 R_E.

Figure 8 shows the calculated distance to the OCB for the three spacecraft in the dawn region with the two Van Allen Probes, RBSP-A (black) and RBSP-B (red) in the southern hemisphere and LANL-97A (blue) in the northern hemisphere. The thick lines show the times at which the spacecraft data indicated they had

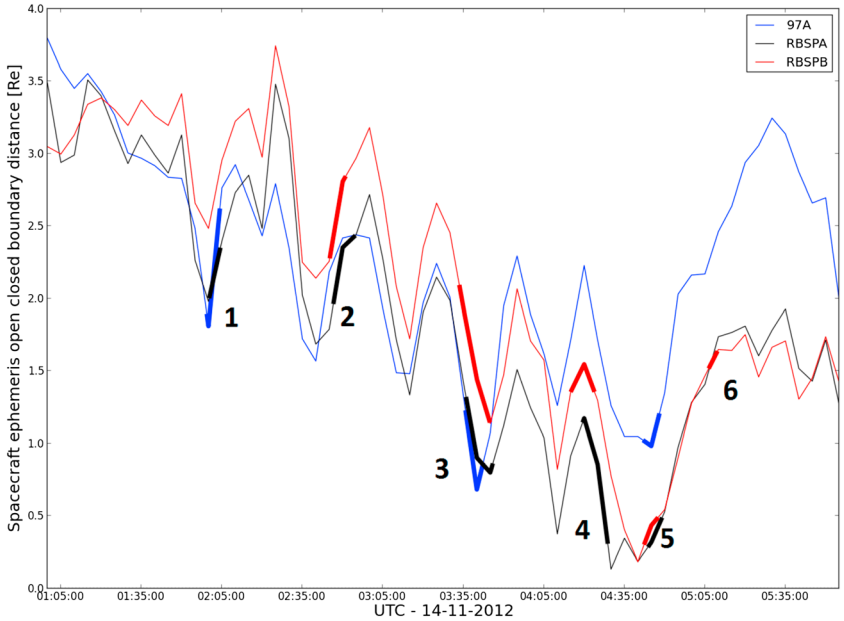

Figure 8. Calculated distances from the RBSP-A (black), RBSP-B (red), and LANL-97A (blue) to the open-closed field line boundary position predicted by CRCM + BATS-R-US. Distances shown are in R_E with negative distance representing when the spacecraft has entered the lobe. Thicker lines show periods where the spacecraft data indicate that it has entered the lobe.

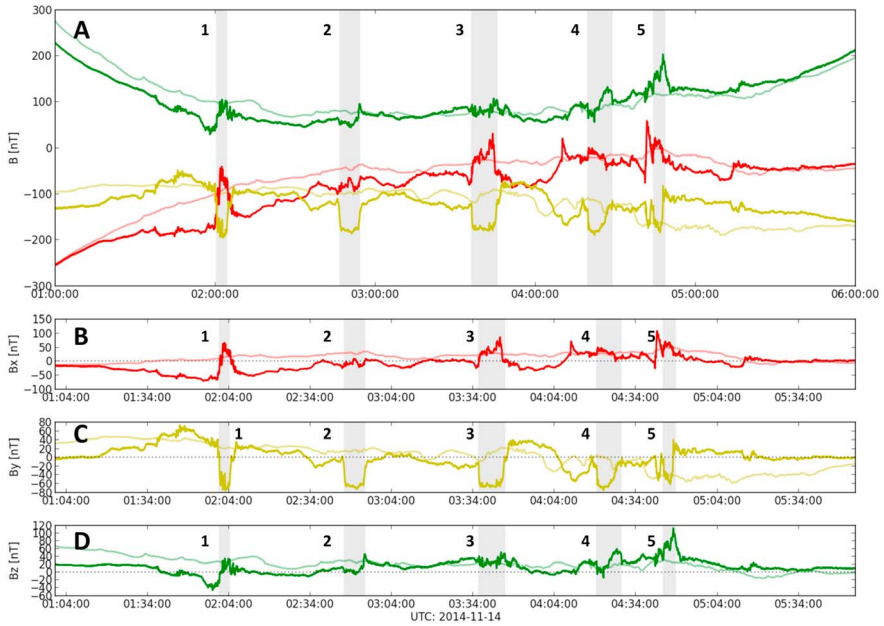

Figure 9. RBSP-A EMFISIS magnetometer data and CRCM + BATS-R-US simulated magnetic field for 0100–0600 14 November 2012. (a) B_x (red), B_y (yellow), and B_z (green) shown. Bold lines show magnetometer data from EMFISIS and light lines show MHD model magnetic field. (b) B_x after removal of TSO4 predicted magnetic field. (c) B_y after removal of TS04 predicted magnetic field. (d) B_z after removal of TS04 predicted magnetic field. Grey-shaded areas show periods when the spacecraft has entered the lobe.

passed into the lobe. No lobe encounters are predicted. Generally, the comparison is not as consistent at dawn, likely because the lobe encounters are shorter and more difficult to reproduce in the model.

For all three spacecraft the model shows both the northern and southern lobe advancing and retreating in a cyclical manner with a period of around half an hour. Events 1, 2, 3, and 5 coincide fairly well with the lobe expansions, occurring at least partially within the minima of the oscillations. Event 4 occurs when the model shows the lobes to be in retreat and is not seen by LANL-97A in the northern hemisphere. Event 6, which is only seen by RBSP-B, occurs after the periodic expansion and contraction has ceased and the model predicts the OCB to be over 1.5 R_E from the spacecraft. There is a clear minimum between events 2 and 3 which does not coincide with a lobe crossing seen by any of the spacecraft. For the 13 lobe encounters seen between the three spacecraft, six of them (~60%) show good agreement with the model prediction, which placed the OCB to within ±1 R_E of the spacecraft. Ten of the events (~75%) occurred when the model predicted an approach of the boundary toward the spacecraft.

As well as the periodic movement of the boundary there is also a steady decrease in the distance to the OCB until 0430 UT where the lobes contract again. This gradual expansion and then faster contraction of the lobes coincides with a steady increase and then decrease in solar wind proton density.

Across both dawn and dusk, 60% of the lobe encounters occurred within ±1 R_E of the predicted position of the OCB. For both the dawn and dusk statistics the closest approach during each encounter was utilized. Considering the relatively short duration of some of the events and the temporal coarseness of the model, this agreement is fairly good and shows the model is at least partially representing the dynamics of the events.

To further understand the lobe encounters we next examine in more detail another critical aspect of their character, that of the magnetic field. It is advantageous to look at fluctuations from the background magnetic field to isolate the stretching that is associated with the lobe encounters. To isolate these fluctuations the expected magnetic field characteristics contained in the ECT ephemeris data, derived from the TS04 model, are subtracted from the magnetometer measurements from EMFISIS. This effectively removes the large-scale changes in the magnetic field and leaves only the signatures associated with the lobe encounters. We note that the TS04 model reproduces the large-scale field for this orbit reasonably

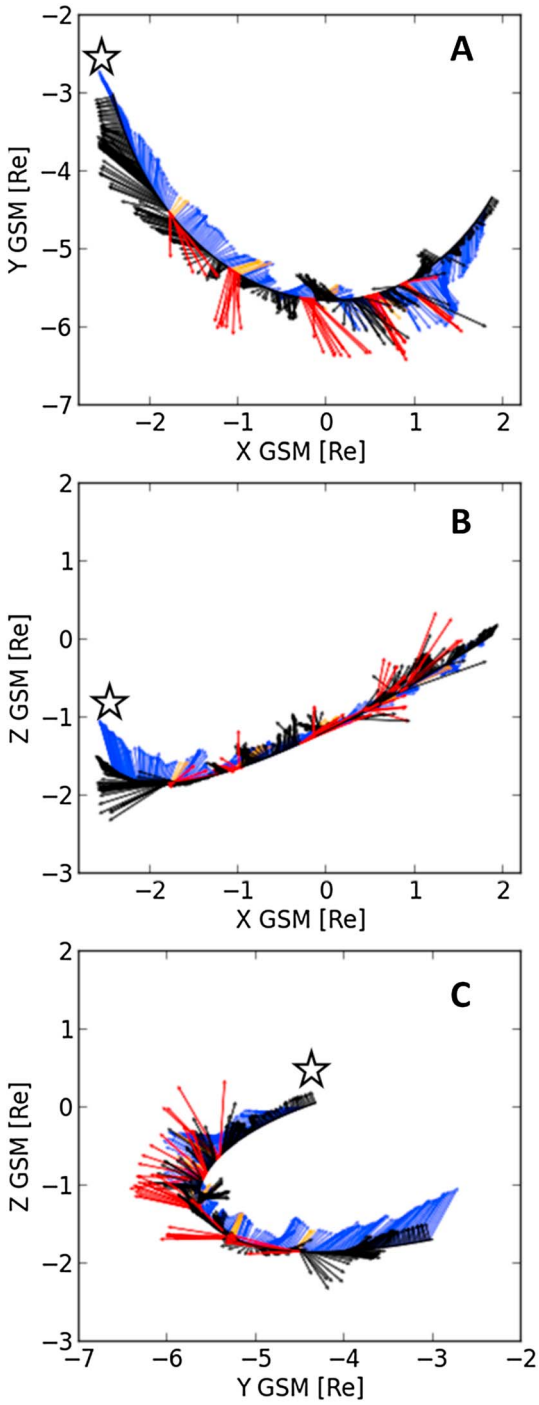

Figure 10. Magnetic field fluctuation vectors derived from RBSP-A EMFISIS magnetometer data and BATS-R-US simulated magnetic field for the period 0100–0600 14 November 2012. Arrows show the direction and relative strength of the magnetic field, plotted along the spacecraft orbit. Black arrows show the magnetic field configuration for RBSP-A EMFISIS with the red arrows marking times when the spacecraft has entered the lobe. The blue arrows show the model magnetic field configuration with the yellow arrows marking times when the spacecraft has entered the lobe. (a–c) *X-Y* GSM, *X-Z* GSM, and *Y-Z* GSM plane, respectively. Stars mark the beginning of each orbit.

well; however, as an average statistical model it does not come close to reproducing the lobe encounters nor should it.

Figure 9 shows the magnetic field fluctuation vectors relative to the nominal TS04 + IGRF from RBSP-A observations (thick lines) and as simulated at the spacecraft position by CRCM + BATS-R-US (thin lines). The top panel shows the magnetic field before the removal of the background and the bottom three after it is removed, with the grey-shaded boxes indicating the lobe encounters.

The lobe encounters seen by RBSP-A are characterized by an increase in negative B_y (~ −60 to −80 nT) seen for all five of the events and an increase in B_x observed for all of the encounters apart from the second. There are changes in B_z during the events, but these are not consistent. Event 1 shows a sharp change of B_z (−50 to 50 nT) at the start of the event, whereas event 2 shows a sharp increase in B_z at the end of the event. Event 3 shows little change, except for a small increase at the end. Event 4 changes from −20 to 50 nT but gradually over the duration of the event. Event 5 shows a large increase in B_z which persists for the duration of the event and peaks at 100 nT. These changes seem to represent the spacecraft encountering a region of highly stretched magnetic field, flattened toward the *x-y* plane.

The magnetic field predicted by the MHD model does not show these large-scale changes. This lack of stretching in the MHD model is consistent with the OCB distance calculations that show the lobe to be greater than 0.5 R_E away for the majority of the events. Outside of the times when the spacecraft encounter the lobes, there are other inconsistencies between the spacecraft and MHD model field topology. The model underestimates B_x and overestimates B_y and B_z, though there is a closer agreement around the later lobe encounters, which is consistent with the model predicting the OCB being very close to the spacecraft for these events.

The stretching of the magnetic field and the differences between the observations and the model field are visualized in Figure 10 for RBSP-A only where the magnetic field (with the background subtracted) is shown as a vector. The arrows show the direction and strength of the magnetic field taken at 1 min intervals and plotted along the spacecraft orbit in GSM

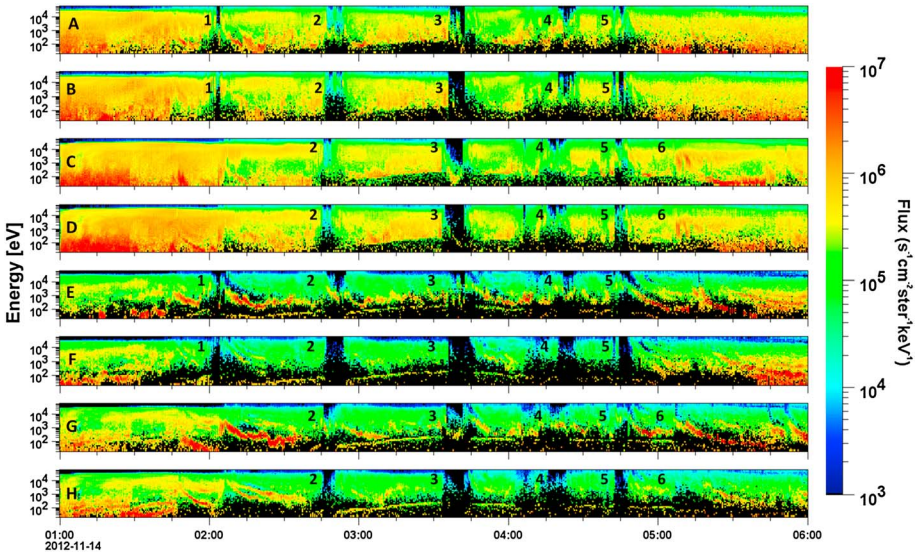

Figure 11. HOPE pitch angle binned differential particle fluxes for the Van Allen Probes between 0100 and 0600, 14 November 2012. (a) RBSP-A 18° pitch angle protons, traveling parallel to the magnetic field (outward from the southern pole). (b) RBSP-A 162° pitch angle protons, traveling antiparallel to the magnetic field (toward the southern pole). (c) RBSP-B 18° pitch angle protons, traveling parallel to the magnetic field (outward from the southern pole). (d) RBSP-B 162° pitch angle protons, traveling antiparallel to the magnetic field (toward the southern pole). (e) RBSP-A 18° pitch angle oxygen ions, traveling parallel to the magnetic field (outward from the southern pole). (f). RBSP-A 162° pitch angle oxygen ions, traveling antiparallel to the magnetic field (toward the southern pole). (g) RBSP-B 18° pitch angle oxygen ions, traveling parallel to the magnetic field (outward from the southern pole). (h). RBSP-B 162° pitch angle oxygen ions, traveling antiparallel to the magnetic field (toward the southern pole).

coordinates, using the same scale factor and same size of range for all panels. Figures 10a–10c show the *X-Y*, *X-Z*, and *Y-Z* planes, respectively, with the black/red arrows showing the field observed by RBSP-A and the blue/yellow arrows that produced by the model. The red and yellow arrows occur within a lobe crossing. This figure illustrates the amount of magnetic field stretching encountered by RBSP-A during each OCB crossing. In Figure 10a the magnetic field is strongly stretched in Y GSM and to a lesser extent in X GSM during each event. Figures 10b and 10c both show that for event 5 there is a large increase in B_z and although there is also a significant B_y component, this dominates the encountered magnetic field. The model field is significantly different to that observed by RBSP-A, both in general and during the lobe encounters. This is consistent with the model placing the spacecraft a significant distance from the lobe for the majority of the events. It can be seen in Figure 10b that the observed and modeled fields converge slightly toward the latter section of the orbit.

4. Discussion

On 14 November 2012, the Van Allen Probes experienced a series of rapid dropouts and then recoveries of plasma ion and electron flux coinciding with the spacecraft encountering a strong, highly stretched magnetic field. These flux dropouts are consistent with the spacecraft moving from the densely populated equatorial region of closed field lines to the tail lobes, which consist of open field lines and have a much sparser particle population.

Pitch angle binned data from the HOPE instrument aboard the Van Allen Probes is used to determine if the variations in pitch angle distribution during the flux dropouts seen is consistent with the spacecraft having encountered the open field lines of the tail lobe. Both protons and oxygen ions are shown in Figure 11 for the 18° (parallel) and 162° (antiparallel) bins. Examination of pitch angle binned data from the HOPE instrument shows that for the parallel field-aligned particles, traveling antisunward from the southern magnetic pole, there are ions of all species present during the flux dropouts. This is consistent with the spacecraft encountering the open field lines of the southern lobe and observing ions traveling from the ionosphere. The presence of oxygen in these ion populations seen during the dropouts is indicative of an

ionospheric source. The flux of oxygen appears to exceed that of hydrogen as would be expected for outflow at these activity levels [*Cully et al.*, 2003].

Similar accelerated structures are encountered by both spacecraft at nearly the same time which indicates a spatially large or rapidly moving structure (the former being more likely) which threads both open and closed regions. Interestingly, there appears to be energy dispersion with the highest energy ionospheric ions detected during the lobe encounter and then lower energy ions being detected later while in the closed field line region. The gap corresponding to the newly open field line devoid of flux appears with a dispersed signature as well at low energies. This may be consistent with the relatively stationary spacecraft encountering the OCB sweeping past it and then returning toward closed field lines. Once on closed field lines again, slow outflowing ions whose traveling time may easily exceed 10 min are still being encountered. Looking roughly at the slow dispersion, the origin of the particles appears consistent with bursty, intense outflow at the ionospheric source. Due to the pitch angle structure these particles may be directly injected from the nightside ionosphere to the region near the spacecraft on both lobe and near-lobe field lines.

There is a shortage of observations and understanding of such ions [e.g., *Walsh et al.*, 2014]. Some estimates indicate that only 10% of the estimated total ion outflow is actually observed in the magnetosphere [*Seki et al.*, 2001]. There are also strong waves detected during the lobe encounters which are described by *Moya et al.* [2015]. The nature of the acceleration mechanism and the source of these dispersed ions are beyond the scope of this paper. Conversely, the antiparallel field-aligned particles which are traveling earthward show comparatively reduced ion populations during the dropouts, especially for the oxygen ions. Observations of both parallel and antiparallel particles are highly indicative that the spacecraft are encountering the open field lines of the southern lobe.

Examination of the spatial and temporal characteristics of the OCB crossings can be used to give insight into the dynamics of the spacecraft encounters with the lobes and the topology of the boundary. The twin Van Allen probes follow near identical orbital paths, with RBSP-A lagging behind by approximately 45 min during the 14 November event. For the four events (2–5) seen by both spacecraft the delay between the two spacecraft observing the lobe is 3–11 min, with RBSP-B encountering and leaving the lobe first each time. There are also two events (1 and 6) seen only by RBSP-A or RBSP-B, respectively.

The near simultaneity of the lobe encounters seen by the two spacecraft clearly implies that it is the OCB that is expanding and then retreating over the spacecraft. The two events seen only by one spacecraft could be a result of the boundary only extending far enough to encounter one of them, smaller-scale topological changes on the boundary causing only one spacecraft to encounter the lobe or most likely a combination of these two scenarios. This conclusion is also supported by the simulated results obtained from CRCM + BATS-R-US. The OCB distance calculations shown in Figure 8 show a periodic advance and retreat of the boundary which coincide fairly well with the spacecraft lobe encounters.

It is worth considering how the orbital positions for each spacecraft may determine whether and when they encounter the lobe for each event. The relative timings of the events for the two Van Allen Probes spacecraft and their spatial separation can be used to constrain the dynamics of the OCB. Three important spatial and temporal factors are as follows: (1) RBSP-B is always at an earlier MLT than RBSP-A, as the direction of their orbits is from midnight to noon for the period examined and B's orbit lags behind A's. (2) For the first three events RBSP-A is closer to the southern lobe in magnetic latitude and at a higher L value than RBSP-B. (3) The last three events occur after the spacecraft have reached apogee, with RBSP-B becoming closer to the southern lobe and higher in L than RBSP-A.

The most simplistic picture for what defines which spacecraft encounters the OCB first would be that the southernmost spacecraft would encounter the southern lobe first as it expanded upward toward the equator. However, for this event RBSP-B encounters the lobe first for all four of the events seen by both spacecraft, even though RBSP-A is actually further southward in magnetic latitude for events 2 and 3. A related possibility is that the OCB is perturbed locally, expanding over the two spacecraft before retreating. In this scenario the spacecraft that enters the lobe first would exit it last, which is inconsistent with what is observed, i.e., RBSP-B both enters and leaves the lobe first for all four events.

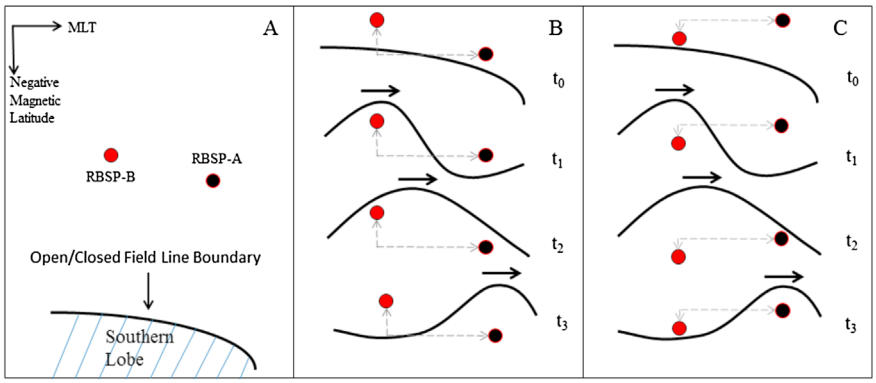

Figure 12. Diagram of possible OCB motion during lobe crossing events. (a) Diagram is drawn in an MLT versus negative magnetic latitude frame. RBSP-A and RBSP-B are represented by black and red circles, respectively. The southern OCB is represented by a black line with the open field lines of the southern lobe below it and the closed field lines of the equatorial region above it. (b and c) An expansion of the boundary moving forward in MLT from the tail, with Figure 12b showing the spacecraft configuration before apogee and Figure 12c the spacecraft configuration after apogee. (b) RBSP-B is closer to the southern magnetic pole than RBSP-A. (c) RBSP-A is closer to the southern magnetic pole. For both Figures 12b and 12c, RBSP-B is always behind RBSP-A in MLT. t_0–t_4 are four representative time steps used to illustrate the motion of the boundary: t_0, neither spacecraft is within the lobe; t_1, the expansion on the OCB has arrived at RBSP-B and it is within the lobe; t_2, the expansion of the OCB now covers both spacecraft; and t_3, the expansion of the OCB has passed RBSP-B and it is now outside the lobe; RBSP-A is still within the lobe.

The diagram in Figure 12 describes a third scenario, which does appear to be consistent with the observations. These observations could be explained by a disturbance or expansion of the boundary, which travels from the tailward direction, always reaching RBSP-B first. Events 1 and 6 only being seen by one of the spacecraft can be explained in this scenario by the disturbance not having sufficient extent in magnetic latitude to reach either RBSP-B or RBSP-A. This is further supported by the relative weakness of these events, which would be consistent with the spacecraft only just encountering the boundary. It is worth noting that the first scenario, a simple expansion of the boundary to lower negative latitudes, is believed to be occurring in combination with that described in Figure 12 to produce the observed phenomena. A global expansion of the lobe is required to bring the OCB close enough to the spacecraft to allow them to observe these smaller-scale perturbations of the boundary.

Open-closed field line boundary distances calculated using CRCM + BATS-R-US have shown some correlation with what is observed by the Van Allen Probes and LANL-GEO spacecraft. For the three spacecraft in the dawn sector (RBSP-A, RBSP-B, and LANL-97A), periodic movements of the boundary toward the spacecraft are predicted, which coincide fairly well with the times of the lobe encounters. This approach and then retreat of the boundary is seen for both the northern and southern lobes simultaneously. This implies that this disturbance of the boundary is a global phenomenon where the expansion of each lobe is being driven by the same source. The model shows the polar caps widening and narrowing in concert, not as expected for the B_y effect. An alternate explanation is that reconnection across the front of the magnetosphere can remove closed flux from both hemispheres symmetrically.

There is an overlying trend in the MHD model prediction of the distance to the lobe for the dawn spacecraft where independent of the periodic motion of the boundary there is a gradual approach of the boundary, from approximately 3 R_E away at 0100 UT to only 1 R_E away by 0400 UT. The OCB then retreats suddenly at around 0430 with the distance to the lobes rising from ~1.0 to 3.5 R_E and ~0.4 to 1.8 R_E, for the northern and southern lobes, respectively. The spacecraft data do not agree with this trend, observing lobe encounters while the model puts the boundary > 1 R_E and also showing no variation in the length or strength of the events which correlates with this gradual approach of the boundary. A possible explanation for this trend in the model is the increase and then rapid decrease in solar wind proton density seen by ACE during the events (peaking around 0400 UT), which would cause a compression of the magnetosphere, bring the lobes down to lower latitudes, and make them more accessible to spacecraft. It is not clear why the observed lobe encounters are not more consistent with these expectations.

The two spacecraft in the southern dusk sector observed lobe encounters of much greater length than those seen in the dawn sector, with the largest being event 8 seen by LANL-080 which lasted 50 min. The MHD model predictions of the distance to the lobe for these spacecraft show a very different picture to that seen in the dawn sector. For the three events that occur before 0400 UT (8, 9, and 11), the model puts the spacecraft either very close to or inside the lobe but with no correlation between the actual lobe crossing times and when the spacecraft crosses the boundary in the model. The MHD model predictions of the distance to the lobe do show that the spacecraft would have access to the lobe during this period, even if it does not show a movement of the boundary for each event.

At approximately 0345 UT the MHD model prediction of the distance to the lobe for both spacecraft rapidly increases to 3.4 and 1.3 R_E for LANL-080 and LANL-01A, respectively. This coincides with a change in direction of IMF B_y seen by ACE, which according to the model proposed by *Moldwin et al*. [1995] would reverse the direction in which the lobes are skewed and cause the southern dusk section of the magnetosphere to have less access to them. Events 10, 12, 13, and 14 all occur after this retreat of the OCB away from the spacecraft, despite the model putting LANL-080 more than 3 R_E away from the lobe. Interestingly there is a clear movement of the boundary toward the spacecraft for the two events seen by LANL-01A which match the event times very well. There are movements of the boundary for the events seen by LANL-080 but they are not as well defined and do not correlate with the spacecraft event times.

5. Conclusion

Between 0200 and 0515 UT on 14 November 2012, the twin Van Allen Probes observed particle dropouts consistent with crossing the open-closed boundary into the lobes. The events occurred on the flank between 4 and 6.6 local time and at altitudes between 5.6 and 6.2 R_E. The events occurred during the main phase of a geomagnetic storm while *Dst* was less than −100 nT, with the IMF being strongly southward ($B_z = -15$nT) and eastward ($B_y = 20$ nT). Observations at geosynchronous orbit also show lobe encounters at the dawn and dusk flanks.

The two spacecraft configuration of the Van Allen Probes is used to constrain the spatial and temporal characteristics of each lobe encounter, allowing analysis of the OCB dynamics during this unique event. We found that the lobe encounters were the result of the boundary moving over the spacecraft. A scenario where an expansion of the OCB propagates from the tail and travels sunward over the two spacecraft seems to fit the timing of the observed entries/exits.

These events have provided a chance to examine the global magnetic field topology in detail using multiple spacecraft and comparing them to an MHD model. The model shows an expansion of the open-flux region of the lobes, bringing the OCB relatively close to these low-latitude spacecraft. The models show a varying boundary location near the spacecraft during this time period, in qualitative agreement with the observation of multiple, quasi-periodic lobe encounters at several of the satellites. A new technique has been developed to quantitatively assess the model boundary's distance from the spacecraft, which can then be compared to the times at which they are observed entering the lobe. This technique found that the model reproduces the motion of the boundary toward and away from the spacecraft at times similar to the events but overestimates the overall distance between the OCB and the spacecraft by as much as 3 R_E, which is significant compared to the model's resolution of 0.125 R_E. This implies that the model qualitatively reproduces the dynamic processes that are causing the OCB to approach and retreat from the spacecraft but does not accurately map the global topology of the magnetosphere during these events.

The measured magnetic field signature shows significant stretching and drastic changes in orientation. The measured field vectors are also compared to the CRCM + BATS-R-US model's prediction of magnetic field strength and direction. There are often significant differences which can be roughly summarized as indicating that the model field is not flattened (in the *y* direction) and dynamic enough. Common tools like empirical models models are built from average behavior and are not suitable for these times.

Spatially large, accelerated ion structures are detected by both spacecraft near simultaneously, with the presence of oxygen indicating that they have an ionospheric source. The outflows are dispersed in energy with the spacecraft encountering the highest energy ions while on open field lines and those with lower

energy once they have returned to closed field lines. This dispersion is consistent with bursty, intense outflow from an ionospheric source. These ion outflows are not well understood, and the Van Allen Probes provide an opportunity to examine their spatial and temporal characteristics, which is beyond the scope of this work but will be a focus for future study.

The open-closed field line boundary is complex in space and time. Magnetic field mapping is extremely challenging for such an event. Further study with different OCB boundary techniques and observations is underway under the auspices of a NSF Geospace Environmental Modeling (GEM) focus group (e.g., http://www.bit.ly/gem_mapping), see also *Hwang et al*. [2014]. It is likely that such mapping issues will be relevant for the multipoint MMS mission and that some of the techniques utilized for this event could be applied to other dynamic processes as well. This event illustrates the complexities of understanding dynamic large-scale topologies during geomagnetic storms. Because of such difficulties, multipoint measurements and a systems approach are necessary to gain understanding.

Acknowledgments

ACE and OMNI teams provided solar wind data through the Space Physics Data Facility of NASA Goddard Space Flight Center. The *SYM-H* indices are provided by Kyoto University World Data Center for Geomagnetism. The authors would like to acknowledge useful discussions with S. Zou, K.-J. Hwang, and J. Fennell. This work was supported by the NASA Van Allen Probes RBSP-ECT project. Work at Los Alamos was performed under the auspices of the U.S. Department of Energy. Part of the research in this paper was supported by NASA Van Allen Probes mission funding. The work of P. Dixon was supported by a studentship from the Science and Technology Funding Council (STFC), UK. HOPE data are available from the RBSP-ECT website (http://www.rbsp-ect.lanl.gov/science/DataDirectories.php) with the following data sets used in this work: Differential plasma fluxes—*rbspb_rel02_ect-hope-sci-L2_20121114_v4.0.0.cdf*, *rbspb_rel02_ect-hope-sci-L2_20121114_v4.0.0.cdf*; pitch angle binned fluxes—*rbspa_rel02_ect-hope-PA-L3_20121114_v5.0.0.cdf*, *rbspb_rel02_ect-hope-PA-L3_20121114_v5.0.0.cdf*; spacecraft ephemeris data—*rbspa_def_MagEphem_TS04-D_20121113_v2.1.0.txt*, *rbspa_def_MagEphem_TS04-D_20121113_v2.1.0.txt*. EMFISIS data are available from http://emfisis.physics.uiowa.edu/data/index with the *rbsp-a_magnetometer_4sec-gsm_emfisis-L3_20121114_v1.3.2.cdf* and *rbsp-b_magnetometer_4sec-gsm_emfisis-L3_20121114_v1.3.2.cdf* data sets used in this work. Data from the SOPA instrument on the LANL-GEO spacecraft are available on request from Geoff Reeves, LANL, US—reeves@lanl.gov. For CRCM + BATS-R-US data used in this work, contact Alex Glocer—alex.glocer-1@nasa.gov.

Yuming Wang thanks Lasse Clausen and two anonymous reviewers for assistance in evaluating this manuscript.

References

Aikio, A. T., T. Pitkänen, A. Kozlovsky, and O. Amm (2006), Method to locate the polar cap boundary in the nightside ionosphere and application to a substorm event, *Ann. Geophys.*, *24*, 1905–1917.

Aikio, A. T., T. Pitkänen, D. Fontaine, I. Dandouras, O. Amm, A. Kozlovsky, A. Vaivdas, and A. Fazakerley (2008), EISCAT and Cluster observations in the vicinity of the dynamical polar cap boundary, *Ann. Geophys.*, *26*, 87–105.

Amm, O. (1997), Ionospheric elementary current systems in spherical coordinates and their application, *J. Geomagn. Geoelectr.*, *49*, 947–955.

Amm, O. (1998), Method of characteristics in spherical geometry applied to a Harang discontinuity situation, *Ann. Geophys.*, *16*, 413–424.

Belian, R. D., G. R. Gisler, T. Cayton, and R. Christensen (1992), High Z energetic particles at geosynchronous orbit during the great solar proton event of October, 1989, *J. Geophys. Res.*, *97*(A11), 16,897–16,906, doi:10.1029/92JA01139.

Blake, J. B., et al. (2013), The Magnetic Electron Ion Spectrometer (MagEIS) instruments aboard the Radiation Belt Storm Probes (RBSP) spacecraft, *Space Sci. Rev.*, *179*(1–4), 383–421, doi:10.1007/s11214-013-9991-8.

Chisham, G., M. P. Freeman, T. Sotirelis, R. A. Greenwald, M. Lester, and J.-P. Villain (2005), A statistical comparison of SuperDARN spectral width boundaries and DMSP particle precipitation boundaries in the morning sector ionosphere, *Ann. Geophys.*, *23*, 733–743.

Clausen, L. B. N., J. B. H. Baker, J. M. Ruohoniemi, S. E. Milan, J. C. Coxon, S. Wing, S. Ohtani, and B. J. Anderson (2013), Temporal and spatial dynamics of the regions 1 and 2 Birkeland currents during substorms, *J. Geophys. Res. Space Physics*, *118*, 3007–3016, doi:10.1002/jgra.50288.

Cully, C. M., E. F. Donovan, A. W. Yau, and G. G. Arkos (2003), Akebono/Suprathermal Mass Spectrometer observations of low-energy ion outflow: Dependence on magnetic activity and solar wind conditions, *J. Geophys. Res.*, *108*(A2), 1093, doi:10.1029/2001JA009200.

De Zeeuw, D. L., S. Sazykin, R. A. Wolf, T. I. Gombosi, A. J. Ridley, and G. Tóth (2004), Coupling of a global MHD code and an inner magnetospheric model: Initial results, *J. Geophys. Res.*, *109*, A12219, doi:10.1029/2003JA010366.

Fennell, J., et al. (1996), CRRES observations of particle flux dropout events, *Adv. Space Res.*, *18*(8), 217–228.

Fennell, J. F., J. B. Blake, J. L. Roeder, R. Sheldon, and H. E. Spence (1997), Tail lobe and open field line region entries at mid to high latitudes, *Adv. Space Res.*, *20*(3), 431–435.

Fok, M., T. E. Moore, J. U. Kozyra, G. C. Ho, and D. C. Hamilton (1995), Three-dimensional ring current decay model, *J. Geophys. Res.*, *100*, 9619–9632, doi:10.1029/94JA03029.

Funsten, H. O., et al. (2013), Helium, Oxygen, Proton, and Electron (HOPE) mass spectrometer for the radiation belt storm probes mission, *Space Sci. Rev.*, *179*(1–4), 423–484, doi:10.1007/s11214-013-9968-7.

Glocer, A., G. Tóth, T. Gombosi, and D. Welling (2009), Modeling ionospheric outflows and their impact on the magnetosphere, initial results, *J. Geophys. Res.*, *114*, A05216, doi:10.1029/2009JA014053.

Glocer, A., M. Fok, X. Meng, G. Toth, N. Buzulukova, S. Chen, and K. Lin (2013), CRCM + BATS-R-US two-way coupling, *J. Geophys. Res. Space Physics*, *118*, 1635–1650, doi:10.1002/jgra.50221.

Hwang, K.-J., et al. (2014), The global context of the 14 November, 2012 storm event, *J. Geophys. Res. Space Physics*, *120*, 1939–1956, doi:10.1002/2014JA020826.

Kabin, K., R. Rankin, G. Rostoker, R. Marchand, I. J. Rae, A. J. Ridley, T. I. Gombosi, C. R. Clauer, and D. L. DeZeeuw (2004), Open-closed field line boundary position: A parametric study using an MHD model, *J. Geophys. Res.*, *109*, A05222, doi:10.1029/2003JA010168.

Kessel, R. L., N. J. Fox, and M. Weiss (2013), The Radiation Belt Storm Probes (RBSP) and space weather, *Space Sci. Rev.*, *179*(1–4), 531–543.

Kletzing, C. A., et al. (2013), The Electric and Magnetic Field Instrument Suite and Integrated Science (EMFISIS) on RBSP, *Space Sci. Rev.*, *179*(1–4), 127–181.

Kopányi, V., and A. Korth (1995), Energetic particle dropouts observed in the morning sector by the geostationary satellite GEOS-2, *Geophys. Res. Lett.*, *22*, 73–76, doi:10.1029/94GL02910.

Mauk, B. H., N. J. Fox, S. G. Kanekal, R. L. Kessel, D. G. Sibeck, and A. Ukhorskiy (2013), Science objectives and rationale for the radiation belt storm probes mission, *Space Sci. Rev.*, *179*(1–4), 3–27.

McComas, D. J., et al. (1993), Magnetospheric plasma analyzer: Initial three-spacecraft observations from geosynchronous orbit, *J. Geophys. Res.*, *98*(A8), 13,453–13,465, doi:10.1029/93JA00726.

McComas, D. J., R. C. Elphic, M. B. Moldwin, and M. F. Thomsen (1994), Plasma observations of magnetopause crossings at geosynchronous orbit, *J. Geophys. Res.*, *99*(A11), 21,249–21,255, doi:10.1029/94JA01094.

Meng, X., G. Toth, A. Glocer, M.-C. Fok, and T. Gombosi (2013), Pressure anisotropy in global magnetospheric simulations: Coupling with ring current models, *J. Geophys. Res. Space Physics*, *118*, 5639–5658, doi:10.1002/jgra.50539.

Mitchell, D. G., et al. (2013), Radiation Belt Storm Probes Ion Composition Experiment (RBSPICE), *Space Sci. Rev.*, *179*(1–4), 263–308.

Moldwin, M. B., S. J. Bame, D. J. McComas, J. Birn, and G. D. Reeves (1995), Flux dropouts of plasma and energetic particles at geosynchronous orbit during large geomagnetic storms: Entry into the lobes, *J. Geophys. Res.*, *100*(A5), 8031–8043, doi:10.1029/94JA03025.

Moldwin, M. B., M. I. Fernandez, H. K. Rassoul, M. F. Thomsen, S. J. Bame, D. J. McComas, and J. F. Fennell (1998), A reexamination of the local time asymmetry of lobe encounters at geosynchronous orbit: CRRES, ATS 5, and LANL observations, *J. Geophys. Res.*, *103*(A5), 9207–9216, doi:10.1029/97JA03728.

Moya, P. S., V. A. Pinto, A. F. Viñas, D. G. Sibeck, W. S. Kurth, G. B. Hospodarsky, and J. R. Wygant (2015), Weak kinetic Alfvén waves turbulence during the 14 November 2012 geomagnetic storm: Van Allen Probes observations, *J. Geophys. Res. Space Physics*, *120*, doi:10.1002/2014JA020281.

Paschmann, G., S. Haaland, and R. Treumann (Eds.) (2003), *Auroral Plasma Physics*, *Space Sci. Ser. ISSI*, vol. 15, Kluwer Acad., Dordrecht.

Rae, I. J., et al. (2004), Comparison of photometer and global MHD determination of the open-closed field line boundary, *J. Geophys. Res.*, *109*, A01204, doi:10.1029/2003JA009968.

Ridley, A. J., T. I. Gombosi, and D. L. De Zeeuw (2004), Ionospheric control of the magnetosphere: Conductance, *Ann. Geophys.*, *22*, 567–584.

Sauvaud, J. A., and J. Winckler (1980), Dynamics of plasma, energetic particles, and fields near synchronous orbit in the nighttime sector during magnetospheric substorms, *J. Geophys. Res.*, *85*(A5), 2043–2056, doi:10.1029/JA085iA05p02043.

Seki, K., R. C. Elphic, M. Hirahara, T. Terasawa, and T. Mukai (2001), On atmospheric loss of oxygen ions from Earth through magnetospheric processes, *Science*, *291*(5510), 1939–1941.

Shue, J.-H., J. K. Chao, H. C. Fu, C. T. Russell, P. Song, K. K. Khurana, and H. J. Singer (1997), A new functional form to study the solar wind control of the magnetopause size and shape, *J. Geophys. Res.*, *102*(A5), 9497–9511, doi:10.1029/97JA00196.

Spence, H. E., et al. (2013), Science goals and overview of the Radiation Belt Storm Probes (RBSP) Energetic Particle, Composition, and Thermal Plasma (ECT) suite on NASA's Van Allen Probes mission, *Space Sci. Rev.*, *179*(1–4), 311–336.

Thomsen, M. F., S. J. Bame, D. J. McComas, M. B. Moldwin, and K. R. Moore (1994), The magnetospheric lobe at geosynchronous orbit, *J. Geophys. Res.*, *99*(A9), 17,283–17,293, doi:10.1029/94JA00423.

Tsyganenko, N. A., and M. I. Sitnov (2005), Modeling the dynamics of the inner magnetosphere during strong geomagnetic storms, *J. Geophys. Res.*, *110*, A03208, doi:10.1029/2004JA010798.

Urban, K. D., A. J. Gerrard, Y. Bhattacharya, A. J. Ridley, L. J. Lanzerotti, and A. T. Weatherwax (2011), Quiet time observations of the open-closed boundary prior to the CIR-induced storm of 9 August 2008, *Space Weather*, *9*, S11001, doi:10.1029/2011SW000688.

Walsh, B. M., J. C. Foster, P. J. Erickson, and D. G. Sibeck (2014), Simultaneous ground- and space-based observations of the plasmaspheric plume and reconnection, *Science*, *343*(6175), 1122–1125.

Wrenn, G. L., J. F. E. Johnson, A. J. Norris, and M. F. Smith (1981), GEOS-2 magnetopause encounters: Low energy (<500 eV) particle measurements, *Adv. Space Res.*, *1*(1), 129–134.